THE TECHNOLOGY OF MODELING DEBRIS CLOUD PRODUCED BY HYPERVELOCITY IMPACT

MA Zhao-xia, HUANG Jie, LIANG Shi-chang, ZHOU Zhi-xuan, REN Lei-sheng, LIU Sen

Hypervelocity Aerodynamics Institute, China Aerodynamics Research and Development Center, Mianyang, P.R. China
Email: HAI@cardc.cn

ABSTRACT

Because of the large amount of debris in a debris cloud, it is hard to achieve a complete description of all the debris by a simple function. One workable approach is to use a group of complete distribution functions and MonteCarlo method to simplify the debris cloud simulation. Enough debris samples are produced by SPH simulation and debris identification program firstly. According to the distribution functions of debris mass, velocity and space angles determined by statistical analysis, the engineering model of debris cloud is set up.

Combining the engineering model and MonteCarlo method, the fast simulation of debris cloud produced by an aluminum projectile impacting an aluminum plate is realized. An application example of the debris cloud engineering model to predict satellite damage caused by space debris impact is given at the end.

1 INTRODUCTION

As there are more and more human activities in space, the amount of space debris increases day by day, and the probability of spacecraft being impacted by space debris also rises [1,2]. When impacted by space debris, the thin-shell structure of the spacecraft can generate debris cloud, which continues to collide with internal equipments and causes damage. To assess the kinetic energy lethality of the debris cloud, it is necessary to understand the details of the debris distribution.

A lot of research has been performed for debris cloud produced by hypervelocity impact. Piekutowski and Schonberg [3,4] studied debris cloud theoretically and especially the characteristics of debris cloud produced by oblique hypervelocity impact. Corvvonato, Destefanis and Faraud [5] studied the debris cloud as a whole and proposed an integral model. Cohen [6] proposed a dynamic model of debris cloud. Zhang Yong-qiang, Guan Gong-shun and Zhang Wei [7] proposed a debris model based on the conservation of momentum, mass and energy, the theory of plane shock wave and thermodynamics. All the above research is valuable. However it is still unable to give debris details.

To obtain the details of debris cloud, a new debris cloud model is proposed based on statistical principles in this paper.

2 DEBRIS CLOUD MODEL

Mass, speed and space angles could characterize a debris, so the mass distribution, speed distribution, space angles distribution and the connection of these distributions could characterize a group of debris.

To found the debris distribution functions and model the debris cloud, a series of numerical simulations are performed to systematically calculate the characteristic data of debris with verified numeric simulation method, then the debris data which are gained from numeric simulation results by a debris identify code named DebrisIde are statistical analysed. Based on the analysis, distribution functions are founded. The scheme of modeling debris cloud is shown in Fig.1.
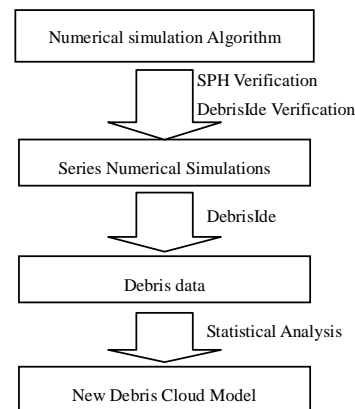

Figure.1. Flowchart of modeling debris cloud

2.1 Numerical Simulation Algorithm

The numerical simulation of debris cloud produced by hypervelocity impact is carried on using SPH method to obtain the mass and movement characteristic parameters of SPH particles at first, then a fragment recognition algorithm is developed to distinguish which SPH particles belong to the same fragment and calculate mass and velocity of the fragment. Thus the fragments data is obtained.

2.1.1 SPH Method

SPH is a Lagrangian technique having the potential to be both efficient and accurate at modelling material deformation. It is also flexible due to the inclusion of specific material models[8]. In addition, SPH is a gridless technique so it does not suffer from the normal problem of grid tangling in large deformation problems. So SPH could simulate the phenomena of continual body structure disintegration, crack, spalling etc.

The foundation of SPH algorithm is the interpolation theory. Various particles' mutual function and physical quantities are described using interpolating functions.

In the SPH method, particle approximation function is described as following:

$$f(x) = \int f(y)W(x-y,h)dy \qquad (1)$$

And $W(x,h)$ is:

$$W(x,h) = \begin{cases} (1-3x^2/2+3x^3/4)/h^d & |x|<1 \\ (2-x)^3/4h^d & 1 \le |x| < 2 \\ 0 & 2 \le |x| \end{cases} \qquad (2)$$

where d is space dimension, h is smooth length.

In computing, the entire area resolves into certain sub-areas. Influencing scope of each particle is a spherical region with the radius of 2h, and then the particles in the lord sub-area and near sub-area are searched. The consumption time is linearly related to the total particle number N.

2.1.2 Fragment Recognition Algorithm

The SPH particle data are obtained from transient state dynamics software. Because it only can provide the information of SPH particles, and can't provide which SPH particles belong to the same fragment. So a code named DebrisIde is developed [9]. DebrisIde uses the breadth first search algorithm and the convex hull solution of large-scale 3D/2D point set to directly obtain the fragment characteristics of the debris cloud, which was simulated by the SPH method.

2.1.3 Algorithm Verification

a SPH Method Verification

The test state is as follows: target thickness is 2.42 mm, the t/D (target-thickness-to-projectile-diameter ratio) is 0.42，the impact velocity is 5.07km/s, normal impact.

The comparison between the test results and the numerical simulation results is shown in Fig.2. The photos of the debris cloud are taken by the serial laser shadow photograph system[10];the size of the hole in target plate of test is 12.3 mm, and the front velocity of the debris cloud obtained by the serial

shadow photographing system is 3.98 km/s；the numerical simulation results show that the hole size is 11.9 mm，and the front velocity is 4.05 km/s. Above the result indicates the numerical simulation result and the test result tally very well.
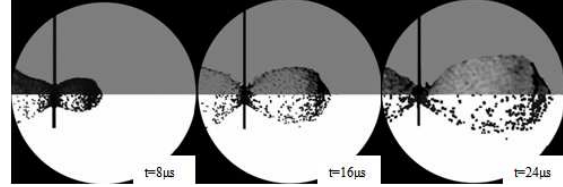

Figure.2 Comparison of debris cloud forms obtained by the test and the numerical simulation(t / D =0.42, V=5.07km/s, θ=0°)

b Fragment Recognition Algorithm Verification

In order to examine the accuracy of DebrisIde, a group of regular geometric bodies with different velocities have been designed, shown in Fig.3.
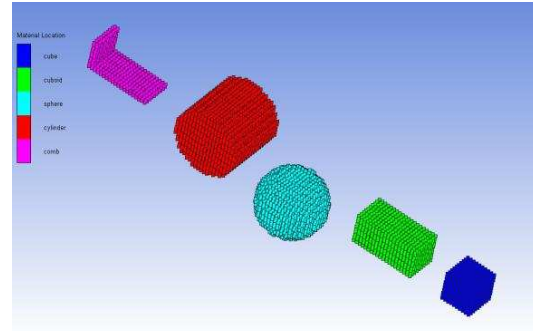

Figure.3 The geometric bodies confirming the fragment recognition algorithm

The material of examination geometry bodies is aluminium with the density of 2.785g/cm3, The SPH particle size is 0.5mm. DebrisIde accurately distinguishes all geometric bodies, and the comparisons are shown in Tab.1. The slight difference between the theoretical mass and recognition mass of two rotating objects is caused by SPH filling area and the geometry body cannot quite same not by DebrisIde. From the above comparison, it is shown that the SPH algorithm and the fragment recognition algorithm are quite reliable.

Table1 Comparison of theory value and recognition values

	mass/mg		
	theory	recognition	Error
cube	348.1	348.1	0.00%
cuboid	696.3	696.3	0.00%
sphere	1458.2	1470.5	0.84%
cylinder	2187.3	2200.2	0.59%
board	208.9	208.9	0.00%

	velocity /km/s		
cube	1.00	1.00	0.00%
cuboid	2.00	2.00	0.00%
sphere	3.00	3.00	0.00%
cylinder	4.00	4.00	0.00%
board	5.00	5.00	0.00%

2.2 New Model of Debris Cloud

Based on numerical simulation results, the mass, velocity and space angles of each debris are obtained by DebrisID program. Then the debris cloud model is built from statistics of debris information. The model includes the velocity of the debris cloud, the distribution of debris mass, velocity, space angles and the relation of different distributions.

The scope of the parameters in this study as follows：The shape of the projectile: sphere；material of the projectile and the target：2A12；impact velocity：3~7 km/s；impact angle：0°~60°；t/D：0.32-0.97. In this study we focus on the debris cloud moving forward. For lower t/D ratios and/or higher velocities, we are yet unable to obtain data suitable for validation of the procedure.

The coordinate used in this study is depicted as follows: in the Cartesian coordinate, the projectile moves along the positive direction of the x axis with velocity of V, and the z axis lies on the target plate. At the impact angle of 0°, the target plate coincides with the yz plane. At the impact angle of θ，the target places as the yz plane rotates counter clockwise around the z axis by an angle θ. The space angles of the debris are represented by α and β，where the α is the angle between the debris position vector and the positive direction of the y axis，and the β is that between the projection of the debris position vector on the xz plane and the negative direction of the z axis（Fig.4）.
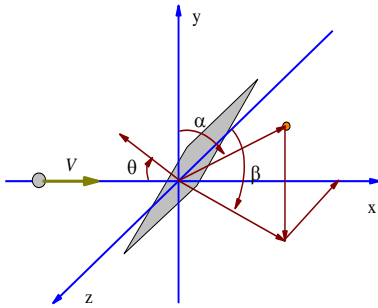

Figure.4   Definition of spatial angles of a debris particle

2.2.1 Debris Cloud Model

a   Velocity of The Debris Cloud

It is assumed that the maximum velocity appears at the debris cloud front, denoted as V_{max}. Fig.5 shows the variation of V_{max} with different impact parameters, where V_{max} decreases monotonously with the increase of t/D. This is due to the lower intensity of the stress wave propagating to the back of the thicker target as the propagation distance increases. When t/D and the impact angle are fixed, the larger the intensity of the shockwave propagating to the target back is, the higher the V_{max} becomes; when t/D and the impact velocity are fixed, the larger the impact angle is, the smaller the projectile velocity projected on the normal direction of the target is, as well as lower shockwave intensity and smaller V_{max}. According to Fig.5, V_{max} can be expressed as Eq. (3), and the coefficients determined by data regression are listed in Tab.2.
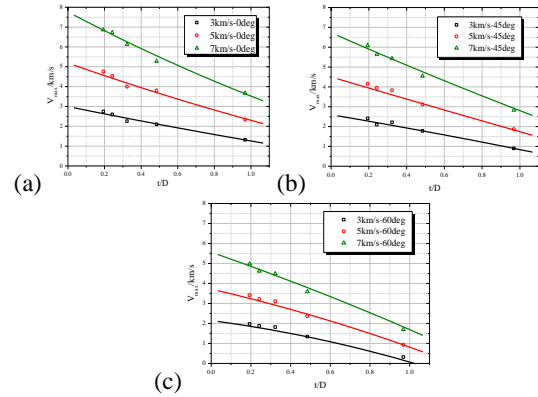

Figure.5   Influence of impact parameters on the velocity of debris cloud front(a.θ=0°, b. θ=45°, c. θ=60°)

$$V_{max}(t/D,V,\theta) = (\sum_{i=0}^{2} ad_i \times (t/D)^i) \times (\sum_{i=0}^{2} av_i \times V^i) \\ \times (\sum_{i=0}^{2} as_i \times \cos(\theta)^i) - k_0 \frac{(t/D)^{k_1}}{\cos(\theta)^{k_2}} \quad (3)$$

Table2   Coefficients in Eq.(3)

i	a_{di}	a_{vi}	a_{si}	k_i
0	0.620	1.142	0.093	0.163
1	-0.389	1.961	0.820	2.058
2	0.063	0.130	-0.324	2.542

b   Distribution of Debris Mass

Define normalized debris mass accumulated number $CN(m)$ as the ratio of the number of debris with mass smaller than m to the total number of debris, that

$$CN(m) = \sum_{m'=0}^{m'=m} n(m') / \sum_{m'=0}^{m'=m_{max}} n(m') \quad (4)$$

where $n(m')$ denotes the number of debris with 4 mass

smaller than m', and m_{max} denotes the maximal mass of debris.

Fig.6 shows the relations of $CN(m)$ with t/D, impact velocity, and impact angle, respectively. It shows that $CN(m)$ increases with the increase of debris mass, but the increase rate drops fast. This means the number of debris with small mass is relatively large, but as the mass increases, the debris number declines. The three impact parameters, t/D, impact velocity and impact angle, have similar influence on $CN(m)$, and none of the factors plays the dominant role. According to Fig.6, $CN(m)$ can be expressed as Eq. (5), and the coefficients determined by data regression are listed in Tab.3.
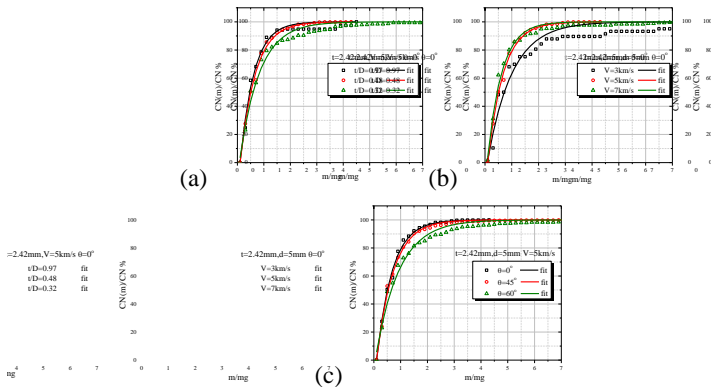

Figure.6 Distribution of debris in mass space(a. the influence of t/D, b. the influence of impact velocity c. the influence of impact angle)

$$CN(m) = 1 - (\sum_{i=0}^{2} ad_i \times (D/t)^i) \times (\sum_{i=0}^{2} av_i \times V^i) \times (\sum_{i=0}^{2} as_i \times \cos \theta^i)$$
$$\times [(\sum_{i=0}^{2} bd_i \times (D/t)^i) \times (\sum_{i=0}^{2} bv_i \times V^i) \times (\sum_{i=0}^{2} bs_i \times \cos \theta^i)] \quad (5)$$

Table3   Coefficients in Eq.(5)

i	a_{di}	a_{vi}	a_{si}
0	6.843	2.579	1.455
1	0.133	0.814	4.984
2	-0.029	-0.075	-2.717
i	b_{di}	b_{vi}	b_{si}
0	0.028	17.024	8.772
1	-0.003	-4.486	-15.998
2	0.001	0.357	8.862

c   Distribution of Debris Velocity

Define normalized debris velocity accumulation number $CN(\nu)$ as the ratio of the number of debris with relative velocity smaller than ν to the total number of debris, that

$$CN(\nu) = \sum_{\nu'=0}^{\nu'=\nu} n(\nu') / \sum_{\nu'=0}^{\nu'=\nu_{max}} n(\nu') \quad (6)$$

Where $CN(\nu')$ is the number of debris with the relative velocity ν', and ν is debris relative velocity, that is the ratio of debris velocity to V_{max}.

Fig.7 shows the influence of t/D, impact velocity and impact angle on the distribution of $CN(\nu)$, respectively. $CN(\nu)$ increases with the increase of ν, and the increase rate is higher with smaller ν'. This means that there are relatively more debris with small relative velocities. As the relative velocity gets larger, $CN(\nu)$ gradually becomes linear in ν space. The comparison of the three plots in Fig.7 indicates that t/D, impact velocity and impact angle have little influence on the distribution of $CN(\nu)$. Accordingly, the distribution function of $CN(\nu)$ in ν space can be expressed as follows:

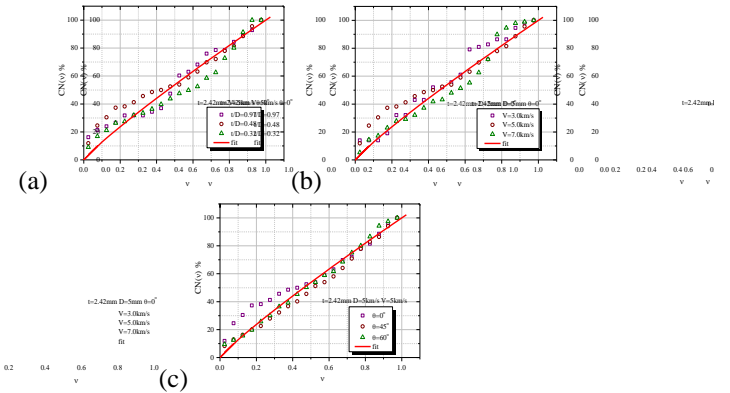$$CN(\nu) = \nu^{0.895} \quad (7)$$

Figure.7 Distribution of debris in velocity space(a. the influence of t/D, b. the influence of impact velocity, c. the influence of impact angle)

d   Distribution of Debris Space Angles

Define $n(\alpha)$ as the percentage of the number of the debris in the angle α out of the total number of the debris, and $n(\beta)$ is similarly defined for the angle β.

In a normal impact, it is a normal distribution with the peak at $\alpha = 90^o$; in an oblique impact, the peak moves rightward from the 90° as the impact angle increases, and the right side of the peak is higher than the left side (Fig.8a), which indicates another peak on the right side of the main peak and the distribution of the debris cloud front in α space as a superposition of two normal distributions (Fig.8b).
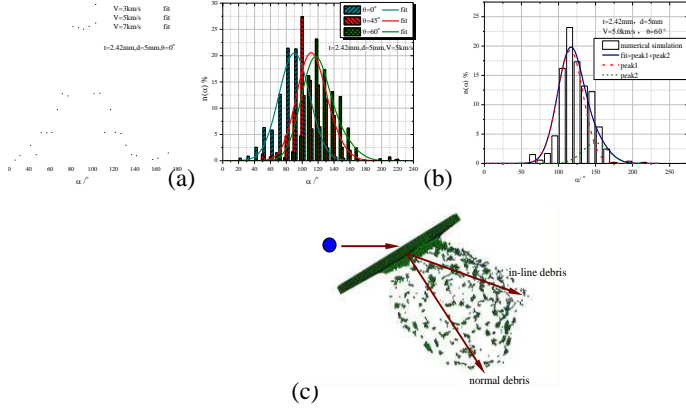
(a)

(b)

(c)

Figure.8 Influence of impact parameters on α angle distribution(a. the influence of impact angle, b. superposition of two normal distributions c. cloud composed two parts)

In a normal impact, the debris particles in the debris cloud front distribute axisymmetrically along the projectile trajectory axis with the majority around the projectile axis, and thus the debris follows a normal distribution which centers at the projectile trajectory axis direction ($\alpha = 90^o$). In an oblique impact, the cloud front is composed of in-line debris and normal debris (Fig.8c). The in-line debris particles come from the crushed pellet. According to the terminal point ballistic theory[11], in an oblique impact the upper and lower parts of the pellet feel uneven forces. After colliding with the target, the projectile trajectory presents an angle to the previous trajectory (under some approximation conditions, the magnitude of the angle can be seen as being proportional to the impact angle), and the peak of the in-line debris cloud deviates from the previous trajectory direction. This leads to the right shift of the debris cloud peak1 from the trajectory direction（ $\alpha = 90^o$ ）in oblique impacts. The normal debris cloud is mainly composed of target debris as some materials of the target are peeled off by the extruding wave generated by the shockwave reflecting on the surface of the target, which is produced in the collision of the pellet and the target. These peeled-off materials move along the normal direction of the target. This constitutes the main part of peak 2. In summary, the debris density distribution function $n(\alpha)$ in α space can be written in the form of Eq. (8).

$$n(\alpha) = \frac{0.85\exp(-2((\alpha-90-17.5\theta)/0.43)^2)}{0.43\sqrt{\pi/2}} + \frac{0.15\exp(-2((\alpha-90-\theta)/17.5)^2)}{17.5\sqrt{\pi/2}} \tag{8}$$

The distribution of $n(\beta)$ is similar to $n(\alpha)$ distribution in normal impacts, with the peak

appearing at $\beta = 90^o$, and the peak width related to t / D , impact velocity as well as impact angle. Express $n(\beta)$ in the form of Eq. (9), and the coefficients w_β is 22.5.

$$n(\beta) = \frac{\exp(-2((\beta-90)/w_\beta)^2)}{w_\beta\sqrt{\pi/2}} \tag{9}$$

e The Relation of Different Distributions

It is not sufficient to describe the debris cloud by only using the distribution functions of debris mass, velocity and space angles. The relations between the three distributions are needed. There is no obvious characteristic feature of the distribution of debris mass in the velocity space, and it can be treated as an even distribution approximately.

It is illustrated in Fig.9a that the space angles are mainly distributed inside the envelope lines in v space, which is related to impact angle θ . In a normal impact, the envelope line is symmetric about $\alpha = 90^o$. In an oblique impact, the debris cloud does not hold that symmetry anymore as the in-line debris separates from the normal debris, and thus the center of the envelope line deviates upward from $\alpha=90^o$, as well as the loss of symmetry of the upper and lower envelope lines. Fig.9b is the distribution of the space angle β in v space, which are all symmetric about $\beta=90^o$. As the impact angle increases, the distribution remains symmetric, but the distribution region enlarges, which results in a more flat and more linear envelope line. According to the distribution characteristics of the debris space angle in the relative velocity space and the interchangeability of α and β in normal impact, the upper and lower envelope lines of α and β can be expressed as Eq. (10):

$$\begin{cases} \alpha_{max}(\theta,v)=g(\theta,v)+f(\theta,v) \\ \alpha_{min}(\theta,v)=g(\theta,v)-f(\theta,v) \\ \beta_{max}(\theta,v)=g(0,v)+f(\theta,v) \\ \beta_{min}(\theta,v)=g(0,v)-f(\theta,v) \end{cases} \tag{10}$$

Where $g(\theta,v)$ and $f(\theta,v)$ can be written as Eq. (11). The coefficients determined by data regression are listed in Tab.4.
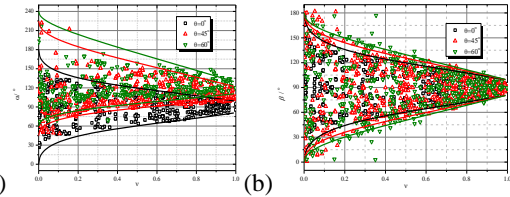

(a)　　　　　　　　　(b)

Fig.9 Distribution of the spatial angle in relative velocity space(a. Distribution of the special

angle α in v space, b. Distribution of the special angle β in v space)

$$\begin{cases} g(\theta,v) = 90 + \theta - \dfrac{\theta}{2}v \\[2mm] f(\theta,v) = \dfrac{90 + p_1 v^{0.5}}{1 + p_2 v + p_3 v^{0.5}} + \\[2mm] (1 - \cos\theta)[90 - kv - \dfrac{90 + p_1 v^{0.5}}{1 + p_2 v + p_3 v^{0.5}}] \end{cases} \qquad (11)$$

Table4   Coefficients in Eq.(11)

p_1	p_2	p_3	k
-83.021	-1.026	0.801	80.997

2.2.2 Debris Cloud Model Verification

a   Verification of Debris Could Shape

According to above debris cloud model, uses Monte-Carlo to sample the method to construct the hypervelocity impact fragment cloud. The scheme of Monte Carlo simulation using the new model is shown in Fig.10.
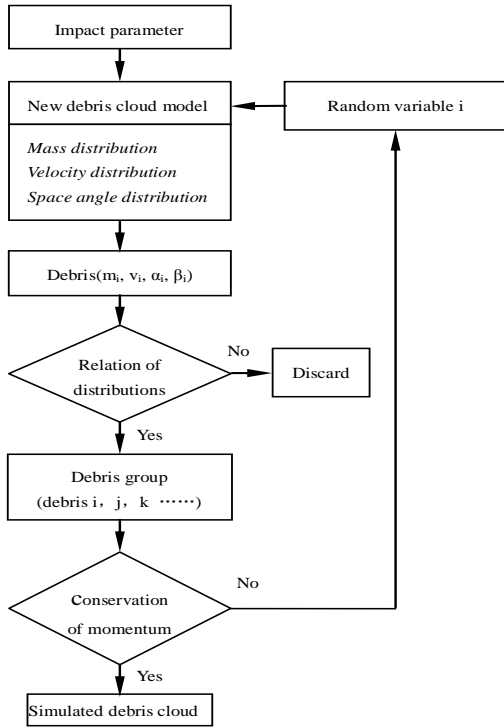

Figure.10   Flowchart of Monte Carlo simulation using the new model

The comparison of the results from the Monte Carlo method, the numerical simulation and the hypervelocity impact test is presented in Fig.11, where the hypervelocity test results are taken from reference [12]. The coordinates of debris are given by the products of debris velocity and time in the result of Monte Carlo and numeric simulation.
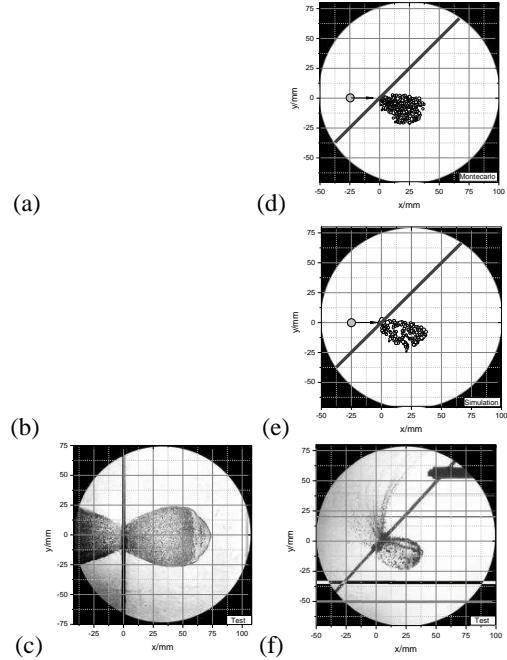

Figure.11   Comparison among the Monte Carlo method, the numerical simulation and the experiment.(a. Monte Carlo, b. Numerical simulation, c. Experiment, impact parameter: t=1.92mm, D=5.0mm, θ=0°, V=6.08km/s, t=15.6μs; d. Monte Carlo, e. Numerical simulation ,f. Experiment impact parameter: t=1.92mm, D=4.0mm, θ=45°, V=4.47km/s, t=14.5μs)

The shape and size of the debris clouds obtained by the three methods at the same time resemble each other: in the normal impact, the debris clouds from the three methods are all close to a spheroidicity, and all travel 75 mm from the impact point after 15.6 μs, with the radiuses expanding to 25 mm; in the oblique impact, the debris clouds all present a 'spoon' shape, and travel 37.5 mm forward and 25 mm downward from the impact point after 14.5 μs.

b   Verification of Debris Could Damage Ability

The comparison of the rear plate's damage derived by Monte Carlo method with that measured in hypervelocity impact test is presented in Fig.12. The material of the target and projectile is aluminium. The target is a Whipple structure and the thickness of both the bumper plate and the rear plate is 3.5mm and the space is 30mm. The diameter of the projectile is 10mm. Normal impact is considered.

The damage of the rear plate is calculated using

perforation formula and ballistic limit equation. Shown in Fig.12，there are a master perforation and some subordinate perforations which are around the master perforation on the rear plate. The calculation shows that the diameter of the master perforation is 20mm and the subordinate perforations are about 2mm in diameter, while it is found in the test that the diameter of the master perforation is 23mm and that of the subordinate perforations is about 2mm. The results are consistent.
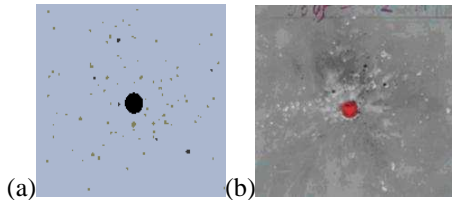

(a)   (b)

Figure.12   Comparison of the rear plates damage(a. Calculation result, b. Test result)

3   APPLICATION

For an application of the new debris cloud model, the damage of satellite impacted by space debris is evaluated. The structure of satellite is hexahedron with the size of 220cm×220cm×170cm. there are a cylinder with the of Φ60cm×220cm , two pressure vessels with the size of Φ50cm and some electronic boxes in the satellite. The thickness of all assembly is 0.5cm and the material is aluminum. The size of space debris is Φ1.0cm ,and the impact velocity is 5km/s.

Evaluation result: After the space debris impacting the shell and electronic box, there are 51 fragments who's diameters bigger than 1mm   produced, those fragments keep flying and impact cylinder, pressure vessels and other electronic boxes (shown in Fig.13a). The upper pressure vessel is impacted by 13 fragments and generator 6 perforations on the front wall. The nether pressure vessel is impacted by 15 fragments and generator 7 perforations on the front wall. There is no perforation on the rear wall for the both pressure vessels (shown in Fig.13b). If the state is evaluated using SPH method, a few days it will take. While using the Monte Carlo method, 18 us it take only.
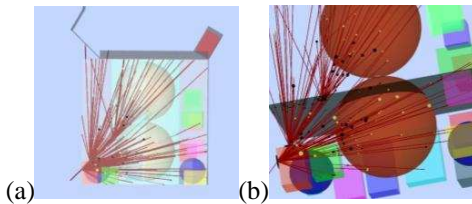

(a)   (b)

Figure.13   Damage evaluation of space debris impact satellite（a．Whole damage, b．Partial damage）

4   SUMMARY

A new debris cloud model is proposed. The model consists of five parts: velocity of the debris cloud, the distribution of debris mass, velocity, space angles and the relation of different distributions.

The fast simulation of the debris cloud produced by hypervelocity impact of a spherical aluminum projectile and an aluminum target is realized. This is achieved by using the Monte Carlo method with the new debris cloud model. The results agree well with those obtained by numerical simulations and tests.

Theoretically, the method presented here can be utilized in the study of the production of debris cloud in hypervelocity impact of other metal materials. The essence of this method is to find appropriate distribution functions. For those debris clouds with the projectile not fully fragmented, the method should be further developed, taking into account the residual fragment.

REFERENCES

[1]   IADC WG3 Members, Protection manual, 2008, http://www.iadc-online.org/Document/Docu/IADC. PM.v3.3.04.04. -2004 .pdf.

[2]   Eric L. Christiansen, Meteoroid/Debris Shielding, NASA Johnson Space Center, Houston, Texas, August 2003.

[3]   A. J. Piekutowski, Formation and Description of Debris Clouds Produced by Hypervelocity Impact, NASA Marshall Space Flight Center, Washington, DC, February 1996.

[4]   W. P. Schonberg, Characterizing Secondary Debris Impact Ejecta, NASA Marshall Space Flight Center, Washington, DC, August 1999.

[5]   E. Corvvonato, R. Destefanis, M. Faraud, Integral Model for the Description of the Debris Cloud Structure and Impact, International Journal of Impact Engineering, 21(2001) 115-128.

[6]   L. J. Cohen, A Debris Cloud Cratering Model, International Journal of Impact Engineering, 17(1995) 229-240.

[7]   Zhang Yong-qiang, Guan Gong-shun, Zhang Wei, Characteristics of Debris Cloud Produced by Normal Impact of Spherical Projectile on Thin Plate Shield, Explosion and Shock Waves, 27(2007) 546-552.

[8]   Century Dynamics. AUTODYN Explicit Software

for Nonlinear Dynamics-SPH User Manual & Tutorial.V4.3. Century Dynamics Inc. 2005

[9]   Liang Shi-chang, LI Yi, Chen Hong, et al．Research on the technique of identifying debris of 3D point set and obtaining character[J]. International Journal of Impact Engineering, IN press, http://dx.doi.org/10.1016/ j.ijimpeng.2012. 07 .004.

[10]   Liu Sen , Xie Ai-min , Huang Jie , Four sequences laser shadowgraph for the visualization of hypervelocity impact debris cloud, Journal of Experiments in Fluid Mechanics, 24(2010) 1-5.

[11]   Sui Yuanshu, Wang Shushan, The influence of the terninal point, National defense industry press, Beijing, 2000.

[12]   Liu Sen, Li Yi, Huang Jie, Hypervelocity impact test results of whipple shield for the validation of numerical simulation. Journal of Astronautics, 26(2005) 505-508.